Research Article

Journal of PeptideScience

Received: 17 June 2008 Revised: 10 September 2008 Accepted: 25 September 2008 Published online in Wiley Interscience: 20 November 2008

(www.interscience.com) DOI 10.1002/psc.1085

FTIR spectroscopic studies on aggregation process of the β-amyloid 11–28 fragment and its variants

Paulina Juszczyk, Aleksandra S. Kołodziejczyk* and Zbigniew Grzonka

Aggregation of Aβ peptides is a seminal event in Alzheimer's disease. Detailed understanding of the Aβ assembly process would facilitate the targeting and design of fibrillogenesis inhibitors. Here, conformational studies using FTIR spectroscopy are presented. As a model peptide, the 11–28 fragment of Aβ was used. This model peptide is known to contain the core region responsible for Aβ aggregation. The structural behavior of the peptide during aggregation provoked by the addition of water to Aβ(11–28) solution in hexafluoroisopropanol was compared with the properties of its variants corresponding to natural, clinically relevant mutants at positions 21–23 (A21G, E22K, E22G, E22Q and D23N). The results showed that the aggregation of the peptides proceeds *via* a helical intermediate, and it is possible that the formation of α-helical structures is preceded by creation of 3_{10}-helix/3_{10}-turn structures. Copyright © 2008 European Peptide Society and John Wiley & Sons, Ltd.

Keywords: Alzheimer's disease; amyloid β; Aβ variants; FTIR spectroscopy; secondary structure studies; aggregation studies

Introduction

Alzheimer's disease (AD), the most common neurodegenerative disorder associated with neuronal loss, is at present one of the most studied pathologies. AD is associated with the progressive deposition of extracellular amyloid in the brain [1,2]. The major component of the plaques and intermediate toxic species is the amyloid β peptide (Aβ), a 39–43 residue long peptide formed by enzymatic cleavage from the much longer amyloid precursor protein (APP) [3]. Missense mutations in the APP gene are usually associated with early-onset familial forms of AD-like diseases (FAD). There is a cluster of mutations around the α-secretase cleavage site which result in Aβ variants changed at positions 21–23. The resultant variants are: A21G (the Flemish variant) [4], E22G (Arctic) [5], E22K (Italian) [6], E22Q (Dutch) [7,8] and D23N (the Iowa variant) [9] (Figure 1). The Aβ peptides may play a crucial pathological role in cerebral amyloid angiopathy (CAA), a common clinical symptom of FAD [10]. The mutations are thought to cause diseases through alteration of APP processing, facilitated fibrilization/protofibrilization of Aβ [5,11], increased cellular toxicity [12], or reduced proteolytic succeptibility [13]. However, several data suggest that the different mutations in APP may manifest their pathogenic effects through different mechanisms [14].

Although the final product in the AD pathogenesis is the insoluble fibril, recent evidence suggests that Aβ oligomers and protofibrils may be the actual cause of neurotoxicity in AD-like diseases [15–19]. Therefore, it is urgent to understand, at the molecular level, not only the structure of insoluble and soluble forms of Aβ, but also the structural changes accompanying their assembly. Structural studies describing the conformation of Aβ peptides in their soluble forms are scarce as these studies are strongly hampered by low solubility in water and by the tendency of the peptides to aggregate. As the structure of Aβ peptides is strongly affected by environmental conditions, studies of the conformational preferences of these peptides in media with different polarity appear to be crucial for shedding light on their intrinsic structural properties related to fibril formation. The aim of this work was to drawn some structural data on the aggregation from conformational studies in a set of mixtures of fluoroalcohol and water.

Although β-amyloid N- and C-truncation alters structural and kinetic features of Aβ fibrillogenesis and morphology of fibrils [20–22], synthetic peptides have proven to be valuable models in the studies of Aβ fibril assembly [23,24]. Recently, we have examined the 11–28 fragment of the Aβ peptide and its clinically relevant variants [25]. The fragment was chosen as it contains the core region responsible for Aβ aggregation, forms fibrils similar to those found for the natural protein [24,26], exerts cellular toxicity *in vitro* and *in vivo* [24,27], and includes residues critical to non-amyloidogenic processing of APP. Our recent work on this Aβ fragment using CD spectroscopy and the thioflavine aggregation test proved it to be a good model for structural studies. Using CD spectroscopy, we found [25] that the aggregation process of Aβ(11–28) variants provoked by the addition of water to their hexafluoroisopropanol (HFIP) solutions is consistent with the hypothesis that a partially folded helix-containing conformer is an intermediate in Aβ fibril assembly [28–30]. To get more insight into early conformational and associative events of the assembly of β-amyloid, we have also studied the aggregation of Aβ(11–28) and its variants by FTIR spectroscopy in promoting aggregation solvent mixtures (HFIP–D_2O) with increasing water content.

CD and infrared spectroscopy are the two methods widely used for determining the secondary structure of Aβ oligomers during the fibrillization process [28,31–33]. In CD spectroscopy, random coil is clearly distinguished from α-helix and β-sheet by

* *Correspondence to: Aleksandra S. Kołodziejczyk, Faculty of Chemistry, University of Gdańsk, Sobieskiego 18, Gdańsk, Poland. E-mail: ola @chem.univ.gda.pl*

Faculty of Chemistry, University of Gdańsk, Sobieskiego 18, Gdańsk, Poland

a characteristic minimum at 200 nm. However, it is difficult to obtain CD data below ~200 nm due to strong scattering of the particles as they associate. Such low-frequency CD data are needed to clearly distinguish α-helix from β-sheet and β-turn secondary structures [34]. FTIR spectroscopy methods are complementary to CD as β-structure is undoubtedly distinguished from α-helix and random coil. The FTIR spectroscopy is characterized by high sensitivity to conformational changes, relatively short acquisition and processing times, the possibility of working in various solvents, and the relatively low sample requirements. Because of its versatility, FTIR spectroscopy has been widely applied to study both proteins and peptides [35–39].

Using this technique, we have studied the (Aβ) 11–28 fragment and its counterparts with all five clinically relevant mutations at positions 21–23, including the Dutch and Iowa variants whose conformational studies were impossible using CD spectroscopy, due to their very fast aggregation.

FTIR Spectroscopy Studies

In recent years, the importance of conformational preference for aggregate formation has been of special interest, as the stability of β-sheet assemblage is necessary for amyloid formation. However, it has been suggested that transient increase of α-helical content may help in the transition from a random coil to a β-sheet structure during fibrillogenesis [29]. In all these processes a hydrogen bond plays a dominant role in deciding the structure of the aggregate. One of the sensitive techniques which gives the opportunity to follow the conformational alterations by hydrogen bond changes is FTIR spectroscopy. Since the aggregation in water is relatively fast as compared to accumulation of the spectra, in the search for experimental conditions that may favor the monitoring of different conformational states accompanying aggregation we resorted to isotropic mixtures of water and fluorinated alcohol with different composition. FTIR spectra of Aβ(11–28) and its variants were registered in pure HFIP and in mixtures of HFIP and phosphate-buffered D_2O (pH = 7.1) with the composition: 90/10, 50/50, 10/90 v/v, respectively. The HFIP-D_2O mixtures were previously used by Szabo [40] and in our CD spectroscopy studies of the same model Aβ peptides [25]. It has been reported that reference spectra in pure HFIP ensure completely stable, ordered solutions of Aβ(11–28), and a uniform, unaggregated state of the peptides [41–43]. All spectra were analysed using GRAMS/32 software (Galactic Enterprises) and the steps of data analysis for an exemplary spectrum are presented in Figure 2. For the analysis, the amide I absorption band (1600–1700 cm^{-1}) was used. The band was proved to be the most sensitive to changes in the hydrogen bonding in peptide/protein molecules and is the most widely used in protein structural studies [35–38].

Since the studies were conducted in HFIP, and its mixtures with D_2O, not in typical aqueous solutions, to avoid ambiguities in band assignment, in some cases we have made use of the results based on CD spectroscopy [25].

E V H H Q K L V F F A E D V G S N K Aβ(11-28) Wt

E V H H Q K L V F F A **K** D V G S N K Aβ(11-28) E22K, Italian mutant

E V H H Q K L V F F A **G** D V G S N K Aβ(11-28) E22G, Arctic mutant

E V H H Q K L V F F A **Q** D V G S N K Aβ(11-28) E22Q, Dutch mutant

E V H H Q K L V F F **G** E D V G S N K Aβ(11-28) A21G, Flemish mutant

E V H H Q K L V F F A E **N** V G S N K Aβ(11-28) D23N, Iowa mutant

Figure 1. Primary structures of the Aβ(11–28) peptides studied by FTIR.

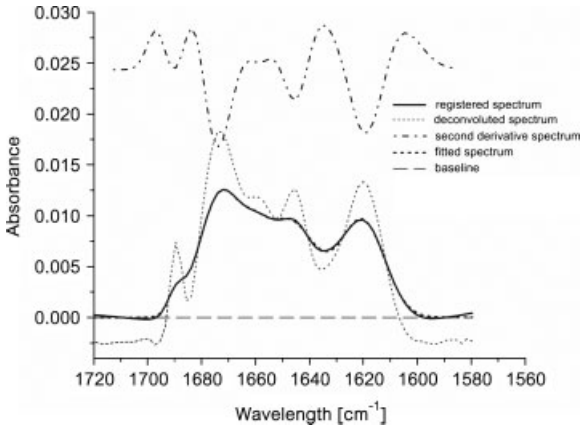

Figure 2. The successive steps of the data analysis of a representative example of FTIR absorbance spectrum (see – e.g. [36]).

Spectra in pure HFIP

Our IR results show some similarities between IR spectra of the examined Aβ variants in HFIP (Figure 3). The greatest resemblance can be seen between the spectra of Aβ(11–28) and its E22K mutant. The analysis of the spectra of Aβ(11–28) wild-type and its E22K variant and their second-derivatives show the main component at 1673 cm^{-1} which may be assigned to a peptide

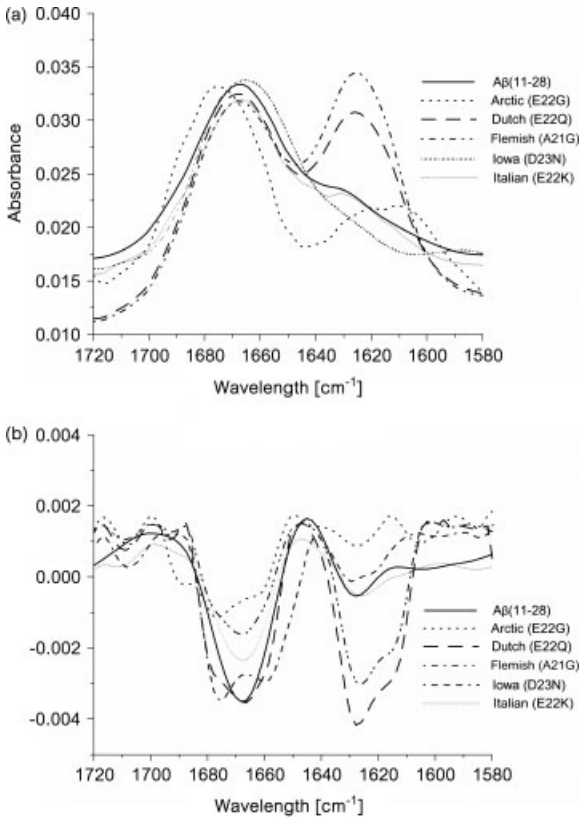

Figure 3. The absorbance FTIR spectra of Aβ(11–28) variants in HFIP (c = 1 mg/ml): (a) the original spectra; (b) the second-derivative spectra.

Table 1. Quantitative analysis of FTIR spectra of Aβ(11–28) and its variants in HFIP

Aβ(11–28)		E22K		D23N		A21G		E22G		E22Q		Structure possible assignment
[cm^{-1}]	(%)	[cm^{-1}]	(%)	[cm^{-1}]	(%)	[cm^{-1}]	(%)	[cm^{-1}]	(%)	[cm^{-1}]	(%)	
								1686	**24**	1680	**15**	**anti-parallel β-sheet**
1673	**77**	1673	**74**	1670	**68**							**α-helix/3$_{10}$helix**
				1655	**11**	1668	**48**	1668	**52**	1665	**41**	**α-helix**
				1642	**17**							**statistical coil**
1627	**23**	1627	**26**	1625	**4**	1624	**44**	1625	**23**	1624	**44**	**β-sheet/turns**
						1612	**4**					**anti-parallel β-sheet**

adopting a helical conformation, or to a combination of structures [35–38] (Table 1). The band could be slightly overestimated due to a residual trifluoroacetate counterion stretching vibration. The band is not seen in the spectra of other Aβ(11–28) variants. This strong, unusual absorption is not in the region typical for helical absorption; however, in some studies strong C=O stretching bands associated with helical structures were reported around 1670 cm^{-1} [40,44]. It is difficult to decide whether the band is due to regular α-helix. Literature data indicate that the α-helical region can be shared by 3$_{10}$-helix conformation [44–47]. The quantitative analysis of the spectra indicates that there is more than 70% of a helical conformation (Table 1). The second component in the spectra of Aβ(11–28) wild-type and its E22K variant was seen at 1627 cm^{-1} and can be attributed to β-sheet structure [35]. Very similar bands at 1624–1625 cm^{-1} were also observed in the spectra of all other variants of Aβ(11–28). In this region, there is striking resemblance between the Flemish and Dutch Aβ(11–28) variants which exhibit very strong bands due to β-sheet structures (1624–1625 cm^{-1}; >40%). The spectrum of the A21G variant shows the band characteristic for helical conformation, similar to those found for the Aβ(11–28) E22G and E22Q peptides. The unusual band at 1612 cm^{-1} was assigned to a minor component of the β-sheet structure band (1624 cm^{-1}). Deconvolution of the spectra of the Arctic and Dutch Aβ(11–28) variants revealed 'high-frequency counterparts' of anti-parallel β-sheet bands [48] (1686 cm^{-1} for E22G and 1680 cm^{-1} for E22Q, Table 1). The peptide Aβ(11–28) D23N was the only one to demonstrate two bands (1670 and 1655 cm^{-1}) which could be assigned to two different helical conformations, or to the helical and β-turn structures. The IR spectrum of this variant differs from the rest of the Aβ peptide spectra also by the presence of the band (1642 cm^{-1}) characteristic for unordered structures (Table 1).

Spectra in HFIP - heavy water mixtures

Addition of water to the solutions of Aβ(11–28) variants in HFIP made the IR spectra more complex. We assumed that their gradual changes reflect mainly structural changes accompanying aggregation provoked by water addition. Since the literature data on FTIR spectra in the applied mixed solvents are scarce, for the interpretation of the results we have used some structural data obtained for the peptides in the same solvent systems with the use of CD spectroscopy [25]. The results of our quantitative analysis of the spectra are presented in Table 2. Analyzing the data, we were aware that the peptide concentration used for FTIR studies was more than 10 times higher than the one used in CD studies, and that the aggregation process in these conditions proceeds much faster.

In all FTIR spectra registered in water–HFIP mixtures, the bands located between 1650 and 1660 cm^{-1} seem to be indicative of the presence of the α-helical conformation. The Arctic (E22G) variant was found to be the one with the greatest amount of this conformation among all examined peptides. Increase of the D_2O content to 90% resulted in the increase of the α-helix content to 42%. A similar tendency was observed for the E22Q variant, but in this case, the increase of α-helix content was lower (8%→ 22%). Quantitative analysis of FTIR spectra for the native Aβ(11–28) peptide and its two variants: E22K and D23N revealed a decrease of α-helix content with increasing D_2O concentration. For some variants we did not observe a typical transient increase of α-helical conformation as it was seen in CD studies for all studied Aβ peptides [25].

Table 2(a). Quantitative analysis of FTIR spectra of Aβ(11–28) in HFIP-D_2O mixtures (c = 1 mg/ml, pH = 7.1)

Aβ(11–28)						Aβ(11–28) E22K						Aβ(11–28) A21G						Possible assignment
10 (%) D_2O		50 (%) D_2O		90 (%) D_2O		10 (%) D_2O		50 (%) D_2O		90 (%) D_2O		10 (%) D_2O		50 (%) D_2O		90 (%) D_2O		
[cm^{-1}]	(%)	[cm^{-1}]	(%)	[cm^{-1}]	(%)	[cm^{-1}]	(%)	[cm^{-1}]	(%)	[cm^{-1}]	(%)	[cm^{-1}]	(%)	[cm^{-1}]	(%)	[cm^{-1}]	(%)	
1685	**2**	1685	**10**	1689	**6**			1691	**3**	1686/92	**6/9**	1690	**1**	1691	**1**	1687	**3**	**anti-parallel β-sheet**
1671	**21**	1672	**22**	1673	**34**			1672	**40**	1673	**29**	1678	**10**			1674	**23**	**turns**
						1666	**46**					1667	**10**	1667	**59**	1661	**20**	**3$_{10}$helix**
1655	**26**	1657	**28**	1657	**12**			1653	**21**	1658	**16**	1659	**3**					**α-helix**
1639	**20**	1641	**11**	1642/47	**6**			1641/48	**15**	1641/48	**15**	1645	**38**	1646	**20**	1645	**26**	**statistical coil**
1629	**11**	1627/30	**17/12**	1633	**14**	1624	**52**	1632	**10**	1627	**11**	1626	**19**	1624	**20**	1632	**1**	**β-sheet**
1618	**20**			1618	**28**	1613	**2**	1610/22	**2/9**	1614	**14**	1614	**19**			1620	**27**	**anti-parallel β-sheet**

Table 2(b).

Aβ(11–28) D23N						Aβ(11–28) E22G						Aβ(11–28) E22Q						Possible assignment
10 (%) D_2O		50 (%) D_2O		90 (%) D_2O		10 (%) D_2O		50 (%) D_2O		90 (%) D_2O		10 (%) D_2O		50 (%) D_2O		90 (%) D_2O		
[cm^{-1}]	(%)	[cm^{-1}]	(%)	[cm^{-1}]	(%)	[cm^{-1}]	(%)	[cm^{-1}]	(%)	[cm^{-1}]	(%)	[cm^{-1}]	(%)	[cm^{-1}]	(%)	[cm^{-1}]	(%)	
1693	**10**	1690	**4**	1689	**3**			1688	**3**	1686	**9**			1692	**1**	1686	**5**	**anti-parallel β-sheet**
1671	**21**	1672	**35**	1673	**28**	1671	**12**	1672	**33**	1673	**18**	1672	**18**	1670	**38**	1673	**35**	**turns**
1655	**20**	1655	**20**	1657	**7**	1654	**29**	1656	**28**	1656	**42**	1658	**8**	1652	**11**	1654	**22**	**α-helix**
1641	**11**	1644	**13**	1641/49	**9**			1641	**21**			1644	**20**	1641	**12**			**statistical coil**
1629	**30**	1635	**5**	1632	**5**	1627	**58**	1628	**10**	1627/34	**10**	1630	**31**	1632	**9**	1638	**9**	**β-sheet**
1615	**8**	1623	**23**	1620	**48**	1614	**2**	1618	**2**	1616	**21**	1616	**23**	1622	**30**	1619	**25**	**anti-parallel β-sheet**

The IR spectra of Aβ(11–28) with the Italian (E22K) and Flemish (A21G) mutations revealed the presence of atypical absorptions at 1666 or 1667 cm^{-1}. In our opinion, these peaks can correspond to 3_{10}-helical conformation or to turns, which typically appear in this region [35]. The 3_{10}-helix and turns were shown to play an essential role in the folding of well-structured α-helix [49,50] and may appear on the aggregation pathway as a form preceding the formation of α-helix. The band corresponding to the atypical helix was seen for the variant with E22K mutation only in the mixture 90%HFIP/10% D_2O; in the mixtures with higher D_2O content the bands appeared at frequencies typical for α-helix. The spectra of the Flemish (A21G) variant showed the band at 1667 cm^{-1} in the mixtures with 10 and 50% of D_2O; however, in the mixture with 90% of D_2O the band appeared at 1661 cm^{-1}. This shift is probably due to the transition to α-helix or to the formation of different helical or turned structures. Specific structures on the aggregation pathway of the A21G variant are probably responsible for lack of bands at wave numbers typical for α-helix (1652–1658 cm^{-1}), which appear in the spectra of all other Aβ(11–28) variants. FTIR analysis of β-structures is complicated by the fact that in this spectroscopy many forms of β-sheets/β-strands give separate bands whose position depends on the strength of hydrogen bonds between strands; moreover, some of them appear in the form of a few components. The bands usually observed between 1610 and 1625 cm^{-1} are indicative of the existence of β-structures with strong, intermolecular, hydrogen bonds, typical for aggregated proteins in which anti-parallel β-sheets are formed. In the FTIR spectra of these structures there are also weak high-frequency components. The precise position of this absorption is difficult to determine, although it is usually found between 1675 and 1695 cm^{-1} [35]. These bands are seen in the spectra of all studied Aβ(11–28) peptides, especially in solvent mixtures with the high content of D_2O (Table 2). In their spectra, the bands are located between 1685 and 1693 cm^{-1}. The variant with the Italian mutation is the one with the lowest content of aggregated β-sheets. On the other hand, the Iowa variant revealed exceptionally high content of these structures (c.a. 48% in the mixture with 90% of D_2O). Aggregated β-sheets are difficult to observe using CD spectroscopy as aggregated forms precipitate from the solution and their formation is manifested only by apparent decrease of β-sheet content [25]. The hydrogen bonds stabilizing typical, loose β-sheets are not as strong as the intermolecular hydrogen bonds stabilizing the extended aggregates, and the amide I frequency for these structures is seen in the analysed spectra at 1624–1638 cm^{-1}. The amount of β-structures corresponding to this absorption has the tendency to diminish with the increase of D_2O content in the solvent used. Simultaneously, the low-frequency peaks (1610–1622 cm^{-1}) corresponding to aggregated β-structures tend to increase with the increase of the water content in the solvent mixtures.

The bands at wave numbers 1638–1649 cm^{-1} were assigned to a statistical coil conformation.

The highest content of this conformation was found in all solvent mixtures for the A21G variant. In the case of this Aβ peptide a random coil structure was very specific and was characterized by bands in a very narrow wave number range (1645–1646 cm^{-1}). For the majority of the Aβ variants the amount of random coil structures significantly diminished with the increase of water content to 90% and with progression of the aggregation process. Apart from the Flemish variant, only the peptide with the Italian mutation revealed a substantial amount of unstructured conformations in the solution with highest water concentration (90% D_20). In the spectra of fast aggregating Aβ(11–28) variants: E22G and E22Q, statistical coil conformations were characterized by bands between 1641 and 1644 cm^{-1} which disappeared completely with the increase of water content. The chiroptical studies of these peptides in the same solvent systems revealed a much higher content of unstructured forms (approx. 30–50%) [25], which is most likely related to a slower aggregation process due to lower peptide concentration used in CD studies.

Discussion

FTIR studies of Aβ(11–28), its clinically relevant variants in HFIP, and its mixtures containing increasing amounts of water (10, 50 and 90% D_2O) enabled us to compare the conformational and aggregational behavior of the Aβ fragment with mutations in position 21–23 in terms of structural changes provoked by the addition of water.

The spectra obtained in HFIP solution revealed significant similarities between the native and the Italian mutant fragments and between the Flemish and Dutch Aβ(11–28) variants. The wild-type fragment and its E22K counterpart were found to be the most helical ones with the prevailing band at an unusual wave number of 1673 cm^{-1}. The spectra in pure HFIP, a strong α-helix inducer [42,51], revealed an unexpectedly high amount of β-sheet conformations (~1625 cm^{-1}) in all variants studied. Moreover, in the case of the Arctic and Dutch variants the band was split and a weak high-frequency component (~1685 cm^{-1}) was observed, suggesting their profound propensity towards anti-parallel β-sheet formation [48]. Although rapid formation of β-structures at the HFIP–water interface was found to be responsible for dramatic acceleration of Aβ aggregation in aqueous HFIP [52], the

presence of a significant amount of β-sheet structures in pure HFIP is intriguing, especially considering the fact that HFIP was proved to disrupt A$\beta\beta$-structures and refold them to α-helices [42].

The unequivocal analysis of the spectra in HFIP–D_2O mixtures was slightly impeded by the lack of reference IR data in these solvents, nevertheless, some general observations could be made.

For the majority of the peptides the increase of the D_2O content in the solvent mixtures resulted in the increase or transient increase of a helical conformation share (bands at 1650–1660 cm^{-1}), supporting the idea of a helix-containing intermediate in the aggregation process of Aβ [28,29]. Although the presence of helical structure in partially unfolded states leading to aggregation was not found to be a fundamental determinant of the ability of peptides to aggregate [52,53], our results indicate that at least in the conditions applied, transition from Aβ monomers to aggregates and fibrils involves formation of a partially folded, helix-containing intermediate. In the spectra of the slow-aggregating Aβ(11–28) variants with E22K and A21G mutations, besides peaks typical of an α-helical conformation (1652–1659 cm^{-1}), unique maxima at ~1666 cm^{-1} were found. The bands can be attributed to 3_{10}-turn/3_{10}-helix conformation, and may imply that this conformation is a folding intermediate to a well-structured α-helix. In the case of the Italian variant, a strong maximum at 1666 cm^{-1} disappeared after further addition of water and the emergence of a peak characteristic of an α-helix (1653–1655 cm^{-1}) was observed. Theoretical and experimental data showed that in moderately sized peptides, the energetic barrier for 3_{10}- to α-helical transition is small and can be easily crossed under a variety of experimental conditions [49,50]. We have also found this type of helical conformation in the structure of the Arctic variant (E22G) of our model peptide. It is very probable that the peptides first form bends and turns which next evolve into 3_{10}-helix segments. These structures can either transform themselves back to turns or further evolve to form α-helix which is more stable than 3_{10}-helix. The fact that 3_{10}-helix formation was seen only in the spectra of Aβ(11–28) E22K and A21G variants is probably related to their lowest aggregative potency found on the basis of the ThT fluorescence assay [25]. For other variants the aggregation in the conditions applied was so fast that transiently formed 3_{10}-helix/turn structures could not be seen, and the formation of α-helix intermediate was only observed.

Lack of frequencies typical of α-helical conformation, and the smallest propensity for fibril formation observed in CD studies [25] in the case of the peptide with the Flemish (A21G) mutation, can reflect different intermediate structures which are probably formed during aggregation of this peptide. It is possible that this Aβ variant cannot reach the α-helical intermediate and forms aggregates with different morphology. This peptide was found to be the one with the highest content of statistical coil structures, manifested by the bands at 1645/1646 cm^{-1}. Our NMR studies of SDS-micelle-bound Aβ(11–28) A21G also revealed that this variant is mainly unstructured with the propensity to form a bent (not helical) structure in the central part [54]. It seems that a small change in the peptide sequence (Ala → Gly) decreases the conformational stability of the whole peptide. Some other studies also report atypical structural features and biological behavior of this Aβ variant [14,55,56]. The presence of bands between 1613 and 1633 cm^{-1} and their 'high-frequency counterparts' (1685–1691 cm^{-1}) in the spectra of the examined peptides reflects the presence of different forms of β-sheet-forming structures. Our experiments showed that, generally, the increase of water content resulted in the decrease of regular, loose β-sheet content (1627–1635 cm^{-1}), and in a pronounced increase of the bands at the lowest frequency (1613–1620 cm^{-1}), manifesting a progressive formation of multi-strand, anti-parallel β-sheet structures. The fastest growth of aggregated forms was observed for the Iowa variant, and a relatively small amount of aggregated β-sheets was seen in the case of the Italian (E22K) variant. The obtained results are in good agreement with our results [25] on relative propensity for aggregation estimated by the ThT assay [57]. Aβ(11–28) E22K was found to be among the variants with the smallest aggregational propensity, and the Iowa (D23N) and Dutch (E22Q) variants were found to be among the fastest aggregating Aβ peptides. Both peptides were also described earlier as Aβ peptides with mutations responsible for enhanced fibrillogenesis and pathogenicity [14].

In the spectra of all peptides studied, bands corresponding to random coil structures were observed (1638–1649 cm^{-1}). A substantial content of unordered forms was found to be characteristic of the Flemish and Italian variants in all solvent mixtures. In both CD and NMR studies, the Flemish peptide was also previously found to be the most unstructured [25,54]. A significant decrease of random coil content with the increase of water content to 90% was found for all other Aβ variants; this feature results from the progress of aggregation provoked by the addition of water and gradual formation of β-sheet structures.

In general, AD-related amyloidogenesis is frequently described in terms of a random coil/α-helix to β-sheet transition [58,59] involving a partially unfolded intermediate. Our IR studies of secondary structure changes were complicated by the fact that the observed conformational changes reflect simultaneous structural transitions accompanying aggregation, insoluble aggregate formation, and conformational changes accompanying the solvent change (HFIP → HFIP–D_2O). In spite of occasionally difficult analysis, the studies confirmed that in HFIP–water mixtures the aggregation proceeds *via* a helical intermediate, and it is possible that the formation of α-helical structures is preceded by creation of 3_{10}-helix/3_{10}-turns. Contrary to the results obtained for full-length Aβ in pure HFIP, our data imply that this solvent is not able to disrupt β-sheet structures of Aβ(11–28), as was observed for Aβ40 and Aβ42 [31]. Our earlier CD studies [25] also led to this conclusion.

Materials and Methods

Peptide Synthesis and Purification

All materials were purchased and used as described earlier [25]. The peptides were synthesized according to the published methods [60] using the standard solid-phase synthesis technique with the Millipore 9050 Plus PepSynthesizer. The details of the synthesis were described earlier [25]. The crude peptides were purified with HPLC using a Vydac C18 semi-preparative column (10 × 250 mm, 5 µm) with 16 ml/min elution and a 120 min linear gradient of 10–40% CH_3CN in 0.08% TFA. The fraction containing pure peptide was lyophilized twice (from the HPLC solvent system and from 0.1 M HCl), and the purity was confirmed by analytical HPLC and by MALDI-TOF analysis.

FTIR Studies

FTIR spectra were recorded on an FS 66 Brucker spectrophotometer with DTGS detector. Each spectrum recorded (average of 32 scans) was collected at a spectral resolution of 4 cm^{-1}. The

sample chamber was continuously purged with nitrogen and all measurements were performed at room temperature. All peptides were prepared for the experiments by dissolution in HFIP (5 mg/ml) in order to have a monomeric sample. Then the solvent was removed by centrifugation *in vacuo*, and the peptides were dissolved in HFIP or mixed solvents: 90% HFIP/10% D_2O, 50% HFIP/50% D_2O, 10% HFIP/90% D_2O (the aqueous solvent was phosphate-buffered D_2O, pH 7.1). FTIR spectra were registered with the use of CaF_2 cuvet (5 µm layer); the final concentration of the peptides was 1 mg/ml. All spectra were vapor-free (no sharp absorption was seen between 1700–1800 cm^{-1}). The spectra were analysed using GRAMS/32 software (version 4.01; Galactic Enterprises). From the spectrum of each sample, a corresponding solvent spectrum was subtracted [61,62]. As an initial step, deconvolution and derivatization were performed (a half-width of 13 cm^{-1} and an enhancement factor K = 5 were applied) to obtain an estimation of the number of discrete absorptions that make up the complex amide I band. For the component analysis, the second-derivative spectra of the amide I region were smoothened with Stavitzky–Golay's 9-point smoothing function [63], and band frequencies were used as starting parameters for curve-fitting analysis. The IR components were described as linear combination of the Gaussian functions. The content of protein secondary structure was calculated from the areas of the bands whose maxima were between 1610 and 1693 cm^{-1}.

Acknowledgements

This work was supported by the Polish Ministry of Science and Higher Education Grant No. 4233/H03/2007/32.

References

1. Selkoe DJ. The cell biology of beta-amyloid precursor protein and presenilin in Alzheimer's disease. *Trends Cell Biol.* 1998; **8**: 447–453.
2. Selkoe DJ. Alzheimer's disease: genes, proteins, and therapy. *Phys. Rev.* 2001; **81**: 741–766.
3. Nunan J, Small DH. Proteolytic processing of the amyloid-beta protein precursor of Alzheimer's disease. *Essays Biochem.* 2002; **38**: 37–49.
4. Hendriks L, Van Duijn CM, Cras P, Cruts M, Van Hul W, van Harskamp F, Warren A, McInnis MG, Antonarakis SE, Martin J-J, Hofman A, Van Broeckhoven C. Presenile dementia and cerebral haemorrhage linked to a mutation at codon 692 of the β – amyloid precursor protein gene. *Nat. Genet.* 1992; **1**: 218–221.
5. Nilsberth C, Westlind-Danielsson A, Eckman CB, Condron MM, Axelman K, Forsell C, Stenh C, Luthman J, Teplow DB, Younkin SG, Näslund J, Lannfelt L. The 'Arctic' APP mutation (E693G) causes Alzheimer's disease by enhanced Aβ protofibril formation. *Nat. Neurosci.* 2001; **4**: 887–893.
6. Rossi G, Macchi G, Porro M, Giaccone G, Bugiani M, Scarpini E, Scarlato G, Molini G, Sasanelli F, Bugiani O, Tagliavini F. Fatal familial insomnia: genetic, neuropathologic and biochemical study of a patient from a new Italian kindred. *Neurology* 1997; **50**: 688–692.
7. Levy E, Carman MD, Fernandez-Madrid IJ, Power MD, Lieberburg I, Van Duinan SG, Bots AM, Luyendijk W, Frangione B. Mutation of the Alzheimer's disease amyloid gene in hereditary cerebral hemorrhage, Dutch type. *Science* 1990; **248**: 1124–1126.
8. Van Broeckhoven C, Haan J, Bakker E, Hardy JA, Van Hul W, Wehnert A, Vegter-Van der Vlis M, Roos RA. Amyloid beta protein precursor gene and hereditary cerebral hemorrhage with amyloidosis (Dutch). *Science* 1990; **248**: 1124–1126.
9. Grabowski TJ, Cho HS, Vonsattel JP, Rebeck GW, Greenberg SM. Novel amyloid precursor protein mutation in an Iowa family with dementia and severe cerebral amyloid angiopathy. *Ann. Neurol.* 2001; **49**: 697–705.
10. Pike CJ, Burdick D, Walencewicz AJ, Glabe CG, Cottman CW. Cultured GABA-immunoreactive neurons are resistant to toxicity induced by beta-amyloid. *J. Neurosci.* 1993; **13**: 1676–1687.
11. Walsh DM, Van Hartley DM, Condron MM, Selkoe DJ, Teplow DB. Amyloid-beta oligomers: their production, toxicity and therapeutic inhibition. *Biochem. J.* 2001; **355**: 869–877.
12. Murakami K, Irie K, Morimoto A, Ohigashi H, Shindo M, Nagao M, Shimizu T, Shirasawa T. Neurotoxicity and physicochemical properties of Aβ mutant peptides from cerebral amyloid angiopathy. *J. Biol. Chem.* 2003; **278**: 46179–46187.
13. Tsubuki S, Takaki Y, Saido TC. Dutch, Flemish, Italian and Arctic mutations of APP and resistance of Aβ to physiologically relevant proteolytic degradation. *Lancet* 2003; **361**: 1957–1958.
14. Van Nostrand WE, Melchor JP, Cho HS, Greenberg SM, Rebeck GW. Pathogenic effects of D23N Iowa mutant amyloid β-protein. *J. Biol. Chem.* 2001; **276**: 32860–32866.
15. Kuo YM, Emmerling MR, Vigo-Pelfrey C, Kasunic TC, Kirkpatrick JB, Murdoch GH, Ball MJ, Roher AE. Morphology and toxicity of Abeta-(1–42) dimer derived from neuritic and vascular amyloid deposits of Alzheimer's disease. *J. Biol. Chem.* 1996; **271**: 4077–4081.
16. Lambert MP, Barlow AK, Chromy BA, Edwards C, Freed R, Liosatos M, Morgan TE, Rozovsky I, Trommer B, Viola KL, Wals P, Zhang C, Finch CE, Krafft GA, Klein WL. Diffusible, nonfibrillar ligands derived from Aβ_{1-42} are potent central nervous system neurotoxins. *Proc. Natl. Acad. Sci. U.S.A.* 1998; **95**: 6448–6453.
17. Klein WL, Krafft GA, Finch CE. Targeting small Aβ oligomers: the solution to an Alzheimer's conundrum. *Trends Neurosci.* 2001; **24**: 219–224.
18. Dahlgren KW, Manelli AM, Stine WB, Baker LK, Kraft GK, LaDu MJ. Oligomeric and fibrillar species of amyloid-beta peptides differentially affect neuronal viability. *J. Biol. Chem.* 2002; **277**: 32046–32053.
19. Kayed R, Head E, Thompson JL, McIntire TM, Milton SC, Cotman CW, Glabe CG. Common structure of soluble amyloid oligomers implies common mechanism of pathogenesis. *Science* 2003; **300**: 486–489.
20. Huang TH, Fraser PE, Chakrabartty A. Fibrillogenesis of Alzheimer Aβ peptides studied by fluorescence energy transfer. *J. Mol. Biol.* 1997; **26**: 214–224.
21. Tjernberg LO, Callaway DJE, Tjernberg A, Hahne S, Lilliehook C, Terenius L, Thyberg J, Nordstedt C. A molecular model of Alzheimer amyloid beta-peptide fibril formation. *J. Biol. Chem.* 1999; **274**: 12619–12625.
22. Päiviö A, Jarvet J, Gräslund A, Lannenfelt L, Westlind-Danielsson A. Unique physicochemical profile of β-amyloid peptide variant Aβ 1-40 E22G protofibrils: conceivable neuropathogenn in Arctic mutant carriers. *J. Mol. Biol.* 2004; **339**: 145–159.
23. Serpell LC. Alzheimer's amyloid fibrils: structure and assembly. *Biochim. Biophys. Acta* 2000; **1502**: 16–30.
24. Rabanal F, Tussel JM, Sastre L, Quintero MR, Cruz M, Grillo D, Pons M, Albericio F, Serratosa J, Giralt E. Structural, kinetic and cytotoxicity aspects of 12–28 β-amyloid protein fragment: a reappraisal. *J. Pept. Sci.* 2002; **8**: 578–588.
25. Juszczyk P, Kołodziejczyk AS, Grzonka Z. Circular dichroism and aggregation studies of amyloid β (11–28) fragment and its variants. *Acta Biochim. Pol.* 2005; **52**: 425–431.
26. Castaño EM, Ghiso J, Prelli F, Gorevic PD, Migheli A, Frangione B. *In vitro* formation of amyloid fibril from two synthetic peptides of different lengths homologous to Alzheimer's disease β-protein. *Biochem. Biophys. Res. Commun.* 1986; **141**: 782–790.
27. Flood JF, Morey JE, Roberts E. An amyloid beta-protein fragment, A beta[12–28], equipotently impairs post-training memory processing when injected into different limbic system structures. *Brain Res.* 1994; **663**: 271–276.
28. Walsh DM, Hartley DM, Kusumoto Y, Fezoui Y, Condron MM, Lomakin A, Benedek GB, Selkoe DJ, Teplow DB. Amyloid-beta oligomers: their production, toxicity and therapeutic inhibition. *J. Biol. Chem.* 1999; **274**: 25945–25952.
29. Kirkitadze MD, Condron MM, Teplow DB. Identification and characterization of key kinetic intermediates in amyloid beta-protein fibrillogenesis. *J. Mol. Biol.* 2001; **312**: 1103–1119.
30. Fezoui Y, Teplow DB. Kinetic studies of amyloid β-protein fibril assembly. *J. Biol. Chem.* 2002; **277**: 36948–36954.
31. Soto C, Castaño EM, Frangione B, Inestrosa NC. The alpha-helical to beta-strand transition in the amino-terminal fragment of the amyloid

Journal of PeptideScience

beta-peptide modulates amyloid formation. *J. Biol. Chem.* 1995; **270**: 3063–3067.
32. Huang THJ, Yang DS, Plaskos NP, Go S, Yip CM, Fraser PE, Chakrabatty A. Structural studies of soluble oligomers of the Alzheimer beta-amyloid peptide. *J. Mol. Biol.* 2000; **297**: 73–87.
33. Benseny-Cases N, Cócera M, Cladera J. Conversion of non-fibrillar beta-sheet oligomers into amyloid fibrils in Alzheimer's disease amyloid peptide aggregation. *Biochem. Biophys. Res. Commun.* 2007; **361**: 916–921.
34. Johnson WC. Analyzing protein circular dichroism spectra for accurate secondary structures. *Proteins: Struct., Funct., Genet.* 1999; **35**: 307–312.
35. Jackson M, Mantsch HH. The use and misuse of FTIR spectroscopy in the determination of protein structure. *Crit. Rev. Biochem. Mol. Biol.* 1995; **30**: 95–120.
36. Haris PI, Chapman D. Analysis of polypeptide and protein structures using Fourier transform infrared spectroscopy. *Methods Mol. Biol.* 1994; **22**: 183–202.
37. Haris PI, Severcan F. FTIR spectroscopic characterization of protein structure in aqueous and non-aqueous media. *J. Mol. Catal., B Enzym.* 1999; **7**: 207–221.
38. Weert M, Haris PI, Hennick WE, Crommelin DJA. Fourier transform infrared spectrometric analysis of protein conformation: effect of sampling method and stress factors. *Anal. Biochem.* 2001; **297**: 160–169.
39. Oberg KA, Fink AL. A new attenuated total reflectance Fourier transform infrared spectroscopy method for the study of proteins in solution. *Anal. Biochem.* 1998; **256**: 92–106.
40. Szabó Z, Jost K, Soós K, Zarandi M, Kiss JT, Penke B. Solvent effect on aggregational properties of β-amyloid polypeptides studied by FT–IR spectroscopy. *J. Mol. Struct.* 1999; **480**: 481–487.
41. Stine WB, Dahlgren KN, Krafft GA, LaDu MJ. *In vitro* characterization of conditions for amyloid-β peptide oligomerization and fibrillogenesis. *J. Biol. Chem.* 2003; **278**: 11612–11622.
42. Vieira EP, Hermel H, Mohwald M. Change and stabilization of the amyloid-β (1-40) secondary structure by fluorocompounds. *Biochim. Biophys. Acta* 2003; **1645**: 6–14.
43. Crescenzi O, Tomaselli S, Guerrini R, Salvadori S, D'Ursi AM, Temussi PA, Picone D. Solution structure of the Alzheimer amyloid beta-peptide (1–42) in an apolar microenvironment. Similarity with a virus fusion domain. *Eur. J. Biochem.* 2002; **269**: 5642–5648.
44. Formaggio F, Bettio A, Moretto A, Crisma M, Toniolo C, Broxterman QB. Disruption of the beta-sheet structure of a protected pentapeptide, related to the beta-amyloid sequence 17–21, induced by a single, helicogenic C(alpha)-tetrasubstituted alpha-amino acid. *J. Pept. Sci.* 2003; **9**: 461–466.
45. Silva RAGD, Yasui SC, Kubelka J, Formaggio F, Crisma M, Toniolo C, Keiderling TA. Discriminating 3(10)- from alpha-helices: vibrational and electronic CD and IR absorption study of related Aib-containing oligopeptides. *Biopolymers* 2002; **65**: 229–243.
46. Maekawa H, Toniolo C, Moretto A, Broxterman QB, Ge N-H. Different spectral signatures of octapeptide 3(10)- and alpha-helices revealed by two-dimensional infrared spectroscopy. *J. Phys. Chem. B* 2006; **110**: 5834–5837.
47. Kubelka J, Silva RAGD, Keiderling TA. Discrimination between peptide 3(10)- and alpha-helices. Theoretical analysis of the impact of alpha-methyl substitution on experimental spectra. *J. Am. Chem. Soc.* 2002; **124**: 5325–5332.
48. Kubelka J, Keiderling TA. Differentiation of beta-sheet-forming structures: ab initio-based simulations of IR absorption and vibrational CD for model peptide and protein beta-sheets. *J. Am. Chem. Soc.* 2001; **123**: 12048–12058.
49. Bolin KA, Millhauser GL. α and 3_{10}: the split personality of polypeptide helices. *Acc. Chem. Res.* 1999; **32**: 1027–1033.
50. Wu X, Wang S. Helix folding of an alanine-based peptide in explicit water. *J. Phys. Chem. B* 2001; **105**: 2227–2235.
51. Gast K, Siemer A, Zirwer D. Fluoroalcohol-induced structural changes of proteins: some aspects of cosolvent-protein interactions. *Eur. Biophys. J.* 2001; **30**: 273–283.
52. Rangachari V, Reed DK, Moore BD, Rosenberry TL. Secondary structure and interfacial aggregation of amyloid-beta(1–40) on sodium dodecyl sulfate micelles. *Biochemistry* 2006; **45**: 8639–8648.
53. Calamai M, Chiti F, Dobson CM. Amyloid fibril formation can proceed from different conformations of a partially unfolded protein. *Biophys. J.* 2005; **89**: 4201–4210.
54. Rodziewicz-Motowidło S, Juszczyk P, Kołodziejczyk AS, Sikorska E, Skwierawska A, Oleszczuk M, Grzonka Z. Conformational solution studies of the SDS micelle-bound 11–28 fragment of two Alzheimer's beta-amyloid variants (E22K and A21G) using CD, NMR, and MD techniques. *Biopolymers* 2007; **87**: 23–39.
55. Walsh DM, Hartley DM, Condron MM, Selkoe DJ, Teplow DB. In vitro studies of amyloid beta-protein fibril assembly and toxicity provide clues to the aetiology of Flemish variant (Ala692 $\rightarrow$ Gly) Alzheimer's disease. *Biochem. J.* 2001; **355**: 869–877.
56. Huet A, Derreumaux P. Impact of the mutation A21G (Flemish variant) on Alzheimer's beta-amyloid dimers by molecular dynamics simulations. *Biophys. J.* 2006; **91**: 3829–3840.
57. LeVine H, III. Thioflavine T interaction with synthetic Alzheimer's disease beta-amyloid peptides: detection of amyloid aggregation in solution. *Protein Sci.* 1993; **2**: 404–410.
58. Mihara H, Takahashi Y, Ueno A. Design of peptides undergoing self-catalytic alpha-to-beta transition and amyloidogenesis. *Biopolymers* 1998; **47**: 83–92.
59. McColl IH, Blanch EW, Gill AC, Rhie AGO, Ritchie MA, Hecht L, Nielsen K, Barron LD. A new perspective on β-sheet structures using vibrational Raman optical activity: from Poly(L-lysine) to the prion protein. *J. Am. Chem. Soc.* 2003; **125**: 10019–10028.
60. Atherton E, Sheppard RC. *Solid Phase Peptide Synthesis: A Practical Approach*. Oxford University Press: Oxford, 1989.
61. Haris PI, Lee DC, Chapman D. A Fourier transform infrared investigation of the structural differences between ribonuclease A and ribonuclease S. *Biochim. Biophys. Acta* 1986; **874**: 255–265.
62. Olinger JM, Hill DN, Jakobsen RJ, Brody RS. Fourier transform infrared studies of ribonuclease in H2O and 2H2O solutions. *Biochim. Biophys. Acta* 1986; **869**: 89–98.
63. Savitzky A, Golay JE. Smoothing and differentiation of data by simplified least squares procedures. *Anal. Biochem.* 1964; **194**: 89–100.

